Optimization and Performance Evaluation of Polymer Inclusion Membrane (PIM) Containing 10% Eugenol-Diallyl Phthalate Copolymer as Carrier for Malachite Green (MG) Transport

Agung Abadi Kiswandono[1*], Rusyda Maulida Khairati[1], Rinawati Rinawati[1], Ni Luh Ratna Gede Juliasih[1], Mita Rilyanti[1], Ilim Ilim[1], Annur Valita Sindiani[1], and Herlian Eriska Putra[2]

[1]*Department of Chemistry, Faculty of Mathematics and Natural Sciences, Universitas Lampung, Jl. Prof. Dr. Ir. Sumantri Brojonegoro, Gedong Meneng, Lampung 35141, Indonesia*

[2]*Research Center for Environment and Clean Technologies, National Research and Innovation Agency, KST BJ Habibie, Setu, Tangerang Selatan 15314, Indonesia*

* ***Corresponding author:***

email: agung.abadi@fmipa.unila.ac.id

Received: July 15, 2025
Accepted: December 16, 2025

DOI: 10.22146/ijc.109274

Abstract: *Malachite green (MG) is a compound commonly used as a dye for silk, leather, wool, cotton, and paper. It is also dangerous for the environment. This study explores the transport of MG using the copolymer (eugenol diallyl phthalate) 10% with the polymer inclusion membrane (PIM) method. The PIM was prepared by dissolving the carrier copolyeugenol diallyl phthalate 10%, polyvinyl chloride (PVC), and dibenzyl ether (DBE) in tetrahydrofuran (THF). This research investigated pH variations in the source phase, HNO_3 concentration in the receiving phase, membrane thickness, carrier concentration, transport duration, and a competition study of MG transport in synthetic wastewater. The concentration of MG after transport was measured using UV-vis spectrophotometry at a wavelength of 614 nm. The results showed that the PIM with 10% copolyeugenol diallyl phthalate effectively transported MG with an efficiency of 88.28% under optimal conditions: a source phase pH of 9, an HNO_3 concentration of 0.75 M, a PIM thickness at T_{54}, and a transport duration of 12 h. The membrane lifetime reached up to 69 days, particularly when $NaNO_3$ salt was added to the source phase.*

Keywords: *eugenol diallyl phthalate; dye; malachite green; polymer inclusion membrane; transport*

■ INTRODUCTION

The rapid development of the industrial sector has not only generated positive impacts on economic growth, social progress, and technological advancements but also led to negative consequences, including increased waste production, particularly in the form of liquid waste. The textile industry, which uses dyes, is a significant contributor to environmental pollution due to its growing industrial activity, which generates substantial waste. Dyes are chemical compounds used to impart color to solutions by absorption or deposition on surfaces. In addition to polluting the environment, dyes can harm ecosystems, threaten biodiversity, and pose risks to human health. The malachite green (MG) dye compound is frequently used in the textile industry. The discharge of waste containing MG causes undesirable coloration of wastewater, reduces sunlight penetration into rivers and lakes, and threatens aquatic ecosystems by causing hypoxia. The nitrogen-containing compounds in MG are also carcinogenic, genotoxic, mutagenic, and teratogenic to living organisms [1].

The typical concentration of MG dye in wastewater is around 0.01 ppm. According to the minimum performance limits set by Commission Decision 2004/25/EC17, the MG level in meat and seafood products is permitted up to 2.0 g/kg. In addition, a report from the Water Research Center for the Department of the Environment, Transport, and the Regions of the

United Kingdom states that the environmental quality standard recommends an average MG concentration of 500 μg/L to protect freshwater life. However, there is no recommended standard for drinking water [2].

Therefore, special treatment of this dye is essential to mitigate its environmental impact, particularly due to the highly hazardous nature of MG. Conventional methods such as adsorption, photocatalytic degradation, and chemical oxidation have been commonly used for treating textile industrial wastewater because they can be applied on a large scale [1,3]. However, these methods often face challenges related to high production, operational, and maintenance costs. The use of adsorption techniques to separate MG with various adsorbents such as zeolite, silica gel, activated carbon, graphite, chitosan, and bentonite is generally considered uneconomical. It requires significant amounts of materials and energy [3]. The methods of adsorption, photocatalytic degradation, and chemical oxidation are commonly used to treat textile wastewater containing MG; adsorption is effective and simple but requires large amounts of materials and energy and does not destroy pollutants, photocatalysis can break down dyes into safer compounds but is slow and dependent on light and costly catalysts, while chemical oxidation works quickly and can eliminate hazardous compounds but requires expensive chemicals and may produce harmful byproducts [4].

One effective way to treat MG waste is through liquid membrane separation technology. There are several main types of liquid membranes, including bulk liquid membrane (BLM), emulsion liquid membrane (ELM), supported liquid membrane (SLM), and polymer inclusion membrane (PIM). Among these, the PIM has emerged as a more stable alternative to other liquid membrane methods for separating and removing MG from wastewater using various carriers [5-7].

The PIM method is often chosen for its wide and selective separation capability, simple operation, low energy requirements, selective extraction of metal and non-metal ions, reduced chemical use, and flexible membrane composition [8]. Liquid membranes contain specific carriers that allow only the target ions or molecules to bind and be transported through them, making them far more selective than conventional methods, such as liquid–liquid extraction [9]. The PIM separation technique involves the use of an effective carrier that is easy to prepare, versatile, stable, and possesses good chemical and mechanical properties. According to Kiswandono et al. [10], PIM shows superior stability compared to other liquid membrane technologies. Additional advantages of PIM include broader interfacial surfaces, high selectivity, durability, efficient separation, and ease of separation. PIM also has a longer lifespan than SLM membranes because its transport mechanism relies on membrane composition and surface homogeneity. Research by Sun et al. [11] supports the use of PIM as an environmentally friendly method that aligns with the principles of green chemistry, as it avoids the use of large quantities of solvents and uses only a relatively small amount of carrier. The transport process in PIM involves three phases: the source phase, which contains the target compound; the membrane phase, which consists of the carrier compound in an organic solvent; and the receiving phase, which serves as the stripping agent for the carrier–target complex. The carrier compound is a key component in the membrane, enabling efficient separation processes [12].

The separation of MG using liquid membranes is based on the differential solubility of MG in aqueous and organic phases. This aligns with the definition of a liquid membrane as a thin semi-permeable layer that separates two liquid or gas phases. The separation principle in liquid membranes is determined not by the membrane itself but by the specific properties of the carrier molecule. The carrier remains within the membrane and can move if dissolved in the liquid phase [13]. The polymer used in the liquid membrane phase must have a high molecular weight, be lipophilic, and possess a structure that allows bonding, interaction, or complexation with the transported compound. One natural material with potential to be developed into a polymer is eugenol.

Eugenol is a chemical component found in clove leaf oil. This compound can be used as a starting material for synthesis because it contains three functional groups:

an allyl group, an ether group, and a phenolic group [14]. With these properties, eugenol can be polymerized into polyeugenol and its derivatives. The resulting polyeugenol meets the criteria for membrane materials due to its high molecular weight and the presence of active –OH groups and benzene rings, making it a promising candidate as a selective transport medium. In this research, copolyeugenol diallyl phthalate was used, which has an active –OH group for the MG transport process.

Copolyeugenol diallyl phthalate is a product of copolymerization modification of eugenol designed to increase the number of active sites on the polymer, which serve as carrier sites in the MG transport process. In MG transport, the carrier facilitates the movement of the target molecule through the membrane. The membrane acts as a selective barrier between two adjacent phases, regulating the transport of chemical components across the membrane [15]. Copolyeugenol diallyl phthalate is superior to pure polyeugenol because the addition of diallyl phthalate creates a more rigid and stable network, improving thermal and chemical stability. It also enhances mechanical strength and resistance to cracking, while providing better surface properties for the efficient adsorption or transport of target compounds, such as MG. In contrast, polyeugenol is softer, less stable, and less effective in such applications [16]. The carrier for this research, copolyeugenol diallyl phthalate, was synthesized by reacting the cross-linking agent diallyl phthalate with boron trifluoride diethyl ether to produce a powdered carrier (copolyeugenol diallyl phthalate), which has a high molecular weight as a requirement for the carrier in the transport process.

PIM is prepared by mixing a carrier, plasticizer, and supporting polymer in a specific solvent, then casting the mixture into a mold to form a thin, stable, and flexible film [1]. The advantages of PIM are based on two main factors: first, the use of base polymers such as polyvinyl chloride (PVC), which is expected to prevent carrier leakage; second, the use of plasticizers, which enhance the stability of the membrane system. PIM offer several benefits, including ease of operation, reduced chemical use, and flexible, selective membrane compositions that support high-efficiency separation processes.

According to Kiswandono et al. [17], PIM with polyeugenol carriers effectively transported MG with an efficiency of 91.30%. This result confirms that the PIM method is effective for the separation of MG. Although various polymer inclusion membranes have been investigated for dye transport, studies utilizing eugenol–diallyl phthalate copolymer as a carrier for MG remain limited. In particular, the effects of membrane thickness, carrier concentration, and stripping agent strength have not been systematically evaluated. Therefore, this study aims to address these gaps by optimizing and assessing the performance of a PIM containing 10% eugenol–diallyl phthalate copolymer for MG transport. Therefore, this study aims to optimize the performance of PIM by examining various parameters, including pH variations in the source phase, HNO_3 concentration in the receiving phase, membrane thickness, carrier concentration, transport duration, and competition study of MG transport in synthetic wastewater. Performance evaluation encompasses variations in plasticizer concentration, salt type, and salt concentration in both the source and receiving phases, as well as reusability tests and transport lifetime testing of MG in synthetic wastewater using PIM with 10% eugenol–diallyl phthalate copolymer (copolyeugenol diallyl phthalate) as the carrier.

■ EXPERIMENTAL SECTION

Materials

The materials used in this study include MG (Sigma-Aldrich M6880), copolyeugenol diallyl phthalate (Sigma-Aldrich 269379), aquabidest (WaterOne Aquadest), PVC (Sigma-Aldrich 81387), dibenzyl ether (DBE, Sigma-Aldrich 33630), tetrahydrofuran (THF, Sigma-Aldrich 34865), nitric acid (HNO_3, Supelco 1.00630), lead(II) carbonate ($PbCO_3$, Sigma-Aldrich 336378), and copper(II) sulfate ($CuSO_4{\cdot}5H_2O$, Sigma-Aldrich C1297).

Instrumentation

The equipment used in this study includes a magnetic stirrer, a magnetic bar, an analytical digital balance (Mettler Toledo AB54-S), a chamber with a diameter of 3.5 cm, a pH meter (pH 60 VioLab pH-Mv-

Orp-T), a membrane mold (5 cm), and a thickness gauge (Mitutoyo 7301). The characterization was performed using scanning electron microscopy (SEM, ZEISS EVO MA 10), Fourier transform infrared spectroscopy (FTIR, Agilent Cary 630), and UV-visible spectrophotometry (Lab Junction LJ-2371).

Procedure

Preparation of PIM

The eugenol–diallyl phthalate copolymer was synthesized by mixing 5.8 g of eugenol with 0.58 g of diallyl phthalate, followed by the addition of 0.25 g of $BF_3{\cdot}O(C_2H_5)_2$ four times, once every hour. The mixture was then stirred until it formed a purple gel. Afterward, 1 mL of methanol was added and left to stand for 1 h. The gel was then washed with chloroform until its pH matched that of distilled water. After reaching a neutral pH, Na_2SO_4 was added, and the mixture was transferred to a mortar and left for approximately 24 to 48 h. Finally, the gel was ground into a powder and stored in a desiccator [10]. PIM was prepared with total weights of 0.27, 0.54, and 1.08 g in a mold equipped with a spin bar. The membrane components consisted of copolyeugenol diallyl phthalate as the carrier, PVC as the base polymer, and DBE as the plasticizer, as shown in Table 1. A volume of 10 mL of THF was added to the membrane components. THF functions as a solvent to homogenize the mixture in the mold. The dissolution process took 30 min. The cast membrane was left to stand at room temperature for 3 days, allowing the solvent to evaporate naturally. The terms T_{27}, T_{54}, and T_{108} refer to the total membrane weights, representing thin, normal, and thick membranes, respectively.

Preparation of the MG stock solution, the synthetic wastewater, and the concentration measurement

The synthetic wastewater containing MG was prepared through a series of steps. First, a 1,000 ppm MG stock solution was prepared by dissolving 1 g of MG in 1 L of bidistilled water. Then, a 25 ppm synthetic wastewater solution containing MG, Pb(II), and Cu(II) was prepared by dissolving 0.0025 g of MG, 0.0098 g of $Pb(NO_3)_2$, and 0.0032 g of $Cu(NO_3)_2$ in a 100 mL volumetric flask, followed by dilution with bidistilled water up to the calibration mark. Prior to measuring the MG concentration, the maximum wavelength of MG at a concentration of 25 ppm was determined using a UV-visible spectrophotometer within the wavelength range of 400–800 nm. Subsequently, the concentration of MG in the standard solution, source phase, and receiving phase was measured by collecting 5 mL of each sample and analyzing the absorbance at the previously determined maximum wavelength [10].

pH variation of MG in the source phase

The pH variation was prepared with the standard-thickness PIM containing the carrier was placed in the center of the transport pipe. Into the pipe, 50 mL of 1 M HNO_3 was added as the receiving phase, and 50 mL of 25 ppm MG solution (with varied pH values of 5.0, 6.0, 7.0, 8.0, and 9.0) was added as the source phase, the pH of the source phase was adjusted by adding 1 M NH_3 to increase the pH and 1 M HCl to decrease the pH. The pipe was sealed and stirred using a magnetic stirrer at 800 rpm for 12 h at room temperature. After stirring, 5 mL samples were taken from both the source and receiving phases, and the MG concentrations were analyzed using a UV-vis spectrophotometer at the maximum wavelength. This parameter was repeated 3 times.

HNO_3 concentration variation in the receiving phase

HNO_3 variation was prepared with the standard-thickness PIM containing the carrier, which was placed in the transport pipe. Then, 50 mL of 25 ppm MG (at optimum pH) was added as the source phase, and 50 mL of HNO_3 with varying concentrations (0.50, 0.75, 1.00, 1.25, and 1.50 M) was added as the receiving phase. The pipe was sealed and stirred for 12 h at 800 rpm at room

Table 1. Composition ratio of membrane-forming components

Membrane	Copolyeugenol diallyl phthalate (g)	PVC (g)	DBE (g)	Total weight (g)
T_{27}	0.0270	0.0864	0.1556	0.2700
T_{54}	0.0540	0.1728	0.3132	0.5400
T_{108}	0.1080	0.3456	0.6264	1.0800

temperature. Afterward, 5 mL samples from both the source and receiving phases were collected and analyzed using a UV-vis spectrophotometer at the determined maximum wavelength. This parameter was repeated 3 times.

Membrane thickness variation

PIM with thickness variations (T_{27} – thin, T_{54} – normal, T_{108} – thick) containing the carrier were placed in the transport pipe. Then, 50 mL of 25 ppm MG (at optimum pH) was added as the source phase, and 50 mL of HNO_3 (at optimum concentration) was added as the receiving phase. The pipe was sealed and stirred for 12 h at 800 rpm at room temperature. After stirring, 5 mL samples from both phases were analyzed using a UV-vis spectrophotometer. This parameter was repeated 3 times.

Carrier concentration variation

Standard-thickness (T_{54}) PIM with varied concentrations of the carrier were placed in the transport pipe, as shown in Table 2. Then, 50 mL of 25 ppm MG (at optimum pH) was added as the source phase, and 50 mL of HNO_3 (at optimum concentration) was added as the receiving phase. The pipe was sealed and stirred for 12 h at 800 rpm at room temperature. Afterward, 5 mL samples were collected from both the source and receiving phases and analyzed using a UV-vis spectrophotometer. This parameter was repeated 3 times.

Transport time variation

The optimum-thickness PIM containing the carrier was placed in the transport pipe. Then, 50 mL of a 25 ppm MG solution (at the optimum pH) was added as the source phase, and 50 mL of HNO_3 (at the optimum concentration) was added as the receiving phase. The component was stirred for different durations: 6, 9, 12, 16, 18, and 24 h at 800 rpm and room temperature. After each time interval, 5 mL samples from both phases were taken and analyzed using a UV-vis spectrophotometer at the previously determined maximum wavelength. This parameter was repeated 3 times.

Membrane characterization

The membrane was characterized to determine its physical, chemical, and morphological properties. Analyses were performed before and after the transport experiments to assess changes caused by the movement of MG. Characterization techniques included FTIR to identify functional groups and SEM to observe the membrane's surface morphology. These analyses provided insights into how the transport process affected the membrane's performance and stability.

■ RESULTS AND DISCUSSION

This study investigates the transport of MG using the PIM method, utilizing copolyeugenol diallyl phthalate as the carrier. Several optimization parameters were examined, including variations in the pH of MG in the source phase, HNO_3 concentration in the receiving phase, different membrane thicknesses, variations in carrier concentrations, variations in transport time, and a competitive transport study of MG in synthetic wastewater. In addition, several evaluation parameters were considered, including variations in plasticizer concentration, types and concentrations of salts in both the source and receiving phases, repeated use of the PIM, and membrane lifespan.

Preparation of PIM

The PIM was prepared in three variations, with total component weights of T_{27} (0.27 g), T_{54} (0.54 g), and T_{108} (1.08 g). The resulting PIM containing 10% copolyeugenol diallyl phthalate is shown in Fig. 1.

The fabricated PIMs were used to study the transport of MG under various conditions in both the source and

Table 2. Carrier concentration variations with a constant mass of PVC and DBE of 0.1728 and 0.3132 g, respectively

Membrane	Copolyeugenol diallyl phthalate (g)	Total weight (g)
1	0.0520	0.0887
2	0.0540	0.1774
3	0.0560	0.2661
4	0.0580	0.3548
5	0.0600	0.4435

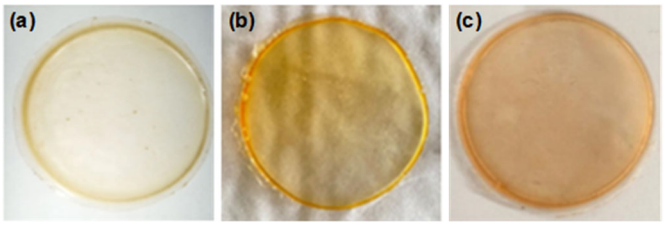

Fig 1. PIM containing 10% copolyeugenol diallyl phthalate: (a) T_{27}, (b) T_{54}, (c) T_{108}

receiving phases. Once the optimal pH in the source phase and the optimal HNO_3 concentration in the receiving phase were determined, variations in membrane thickness were tested to identify the most effective thickness for MG transport. The most optimal PIM was then used in MG transport experiments with varying transport times. This step aimed to determine the best conditions for MG transport using PIM. The thickness of each PIM was measured, and the results are presented in Table 3.

Effect of pH Variation in the Source Phase on MG Transport

This study evaluated the effect of the pH of the MG solution in the source phase on transport efficiency, with tested pH values of 5, 6, 7, 8, and 9. pH serves as a key factor in this study, acting as an indicator that can influence diffusion through the membrane due to the proton concentration gradient between the source and receiving phases. The effect of source-phase pH on MG transport is shown in Fig. 2.

The graph in Fig. 2(a) shows the variation in the amount of MG transported as pH changes. The 10% copolyeugenol diallyl phthalate liquid membrane has been shown to be effective in transporting MG. At this pH, MG tends to exist in a neutral molecular form, allowing it to form more hydrogen bonds. Additionally, the target compound's higher solubility in the organic phase enhances π-π interactions and hydrogen bonding between MG and the carrier in the membrane phase. These increased interactions promote greater MG transport [18].

The FTIR spectra in Fig. 2(b) show changes in the characteristics of the functional groups of MG before and after the transport process using the membrane. In the spectra before transport (black curve), there is a typical absorption at a wavenumber of 3647 cm^{-1} indicating the presence of free –OH groups, as well as a band at 2929 cm^{-1} indicating aliphatic C–H stretching.

Table 3. Total component mass, average membrane mass, and average PIM thickness before transport

Membrane	Total component mass (g)	Average membrane mass (g)	Average membrane thickness (mm)
T_{27}	0.027	0.2518	0.14
T_{54}	0.054	0.4721	0.33
T_{108}	0.108	0.9822	0.41

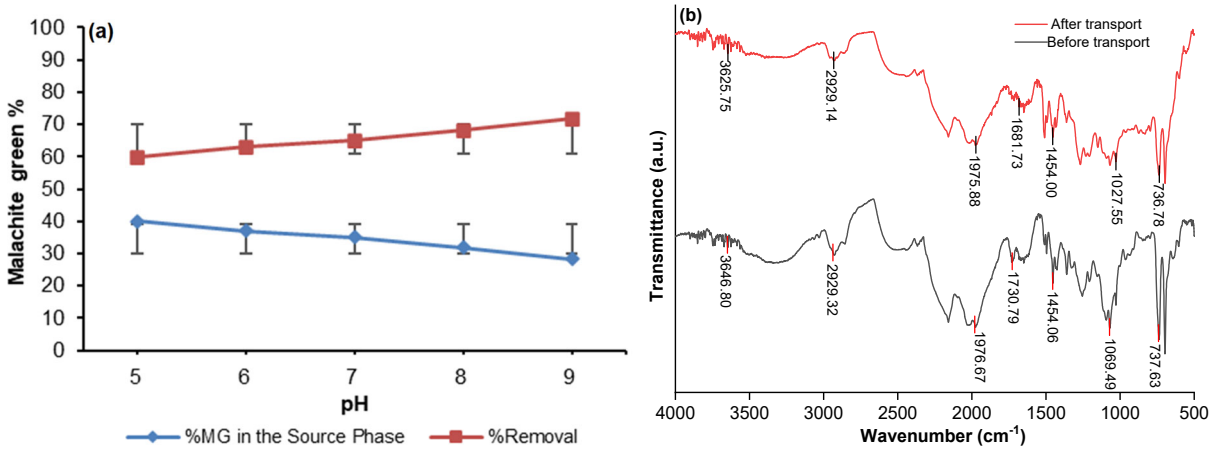

Fig 2. (a) Effect of MG pH in the source phase on MG transport and (b) FTIR spectra of the membrane at different pH variations

After transport with pH variations (red curve), there is a shift and change in band intensity, such as at 1682 cm^{-1}, related to aromatic C=C stretching, and at 1028 cm^{-1}, indicating interactions with membrane components.

According to Ashraf et al. [19], the transport of MG through supported liquid membranes is strongly influenced by the pH of the feed phase, where higher pH conditions significantly enhance dye permeation and transport efficiency. The low efficiency is associated with the high proton concentration at a more acidic pH, which hampers the movement of MG molecules because free protons are more readily transported toward the basic receiving phase. Moreover, the excess protons in the source phase can protonate the membrane, reducing the effectiveness of interactions between MG and the carrier. This triggers competition among MG molecules to bind the carrier, resulting in fewer MG molecules being successfully transported [20].

A similar trend was observed at pH 7 and 8, where the amount of MG transported to the receiving phase increased but still did not exceed the transport efficiency at pH 9, which was identified as the optimal condition in this pH variation experiment [21]. Stated that a neutral to slightly basic source phase pH provides more optimal transport results, whereas acidic pH tends to reduce transport efficiency. These results support the importance of optimizing chemical conditions, particularly pH and acid concentration, in liquid membrane systems to achieve high separation efficiency [22].

Effect of Variations in HNO_3 Concentration in the Receiving Phase on MG Transport

This study examined the effect of receiving phase concentration as one of the key factors influencing MG's ability to pass through the membrane phase. The movement of MG toward the receiving phase is driven by the concentration gradient between the source and receiving phases, which creates a transport force. In this system, the solution in the receiving phase acts as a solvent for the target compound. Therefore, the concentration of the receiving phase is a crucial variable in MG transport studies.

In this experiment, HNO_3 was used as the receiving phase with concentrations of 0.50, 0.75, 1.0, 1.25, and 1.5 M. The transport process was conducted at the optimal source-phase pH of 9. Based on the experimental results, the highest MG transport efficiency was achieved at an HNO_3 concentration of 0.75 M, with a removal percentage (%removal) of 85.18%. A visualization of the effect of HNO_3 concentration on MG transport efficiency is shown in Fig. 3.

Fig. 3(a) shows that the %removal fluctuates, increasing and decreasing with the HNO_3 concentration. The optimum condition was achieved at an HNO_3 concentration of 0.75 M. The percentage of MG removal increased within the concentration range of 0.50–0.75 M, but decreased when the HNO_3 concentration was raised to 1.0–1.5 M. This decline is attributed to the

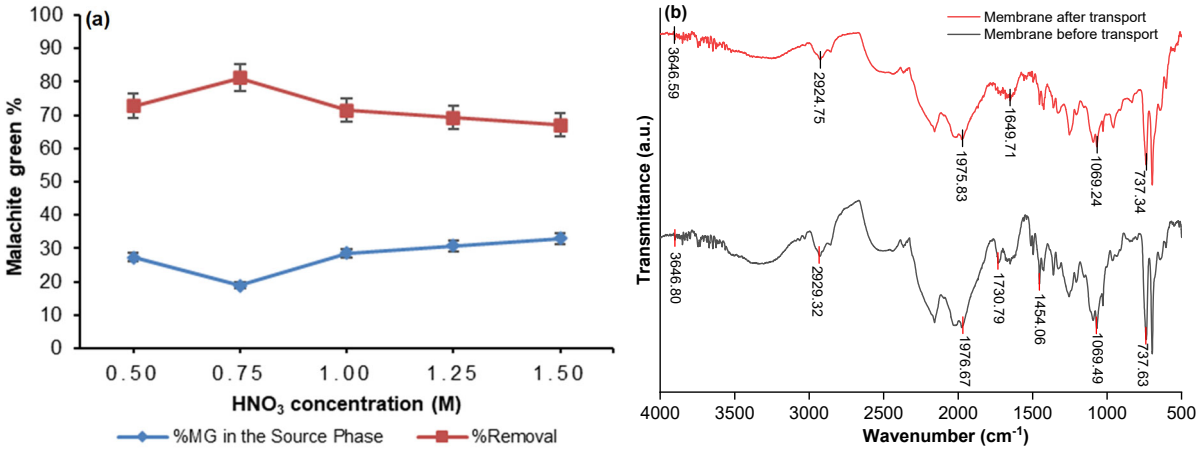

Fig 3. (a) Effect of HNO_3 concentration in the receiving phase on the transported MG concentration and (b) FTIR spectra of the membrane at varying HNO_3 concentrations in the receiving phase

dissociation of HNO_3 in the receiving phase into its ions, namely NO_3^- and H_3O^+ ions, which affect the MG transport process. Additionally, at non-optimal concentrations, leaching may occur at the membrane's active sites, reducing their number and thus hindering transport efficiency. Higher HNO_3 concentrations make it more difficult for the target compound to migrate to the receiving phase due to increased acidity, which causes an imbalance between the release of the target compound and the level of NO_3^- and H_3O^+ ions in the receiving phase [23].

At higher HNO_3 concentrations in the receiving phase, the transport efficiency of MG decreases due to several contributing mechanisms. First, the dissociation of HNO_3 into H_3O^+ and NO_3^- increases ion competition near the membrane, reducing the concentration gradient between the donor and receiving phases and slowing the MG transport rate [24]. Second, excessive acid concentration can lead to saturation of the carrier binding sites in the membrane, limiting further MG binding capacity [25]. Additionally, the excess protons can accelerate back-diffusion into the donor phase, weakening the driving force for transport and potentially hindering the release of MG from the carrier complex, thereby reducing overall transport efficiency [26].

Fig. 3(b) shows FTIR spectra comparing the chemical characteristics of the liquid membrane before and after MG dye transport at various HNO_3 concentration in the acceptor phase. The spectrum before transport (a) displays characteristic absorption bands at 3647 cm^{-1}, which are associated with O–H stretching vibrations, 2929 cm^{-1} corresponding to C–H stretching of alkyl groups, and a band at 1976 cm^{-1} that is presumed to be a combination band or overtone of organic compounds. In addition, the band at 1510 cm^{-1} indicates the presence of aromatic double-bond stretching, possibly originating from MG that has not been completely transported, while the band at 1069 cm^{-1} suggests C–N stretching or bonds related to amine compounds.

After the transport process, as observed in spectrum (a), changes in intensity and slight shifts in wavenumber are evident, such as the emergence of a stronger band at 1650 cm^{-1}, indicating an increased concentration of aromatic groups from MG in the receiving phase. Furthermore, the enhanced bands at 2925 and 1069 cm^{-1} suggest interactions between MG and the membrane components, influenced by the acidic conditions of HNO_3. These changes indicate that the transport process occurred effectively, with MG successfully passing through the liquid membrane and accumulating in the receiving phase.

Effect of Variations in PIM Thickness on MG Transport

In this study, membrane thickness was influenced by several factors, including variations in the total weight of the membrane components, potentially resulting in differences in the final membrane thickness. PIMs were fabricated in three thickness variations: T_{27}, T_{54}, and T_{108}, with total component weights of 0.27, 0.54, and 1.08 g, respectively. It is expected that an increase in the amount of carrier in the membrane, such as –OH groups, along with higher amounts of the main polymer (PVC) and the plasticizer DBE, would enhance the transport efficiency.

At this stage, the MG transport process for each membrane thickness was carried out at the previously determined optimum source-phase pH and HNO_3 concentration in the receiving phase. The effect of membrane thickness on transport is shown in Fig. 4. Fig. 4(a) shows that the optimal membrane thickness for MG transport is T_{54}, with a transport percentage of 85.70%. This high efficiency is attributed to the effective interaction between MG molecules and the carrier. In comparison, the MG transport percentages for membrane thicknesses T_{27} and T_{108} were 74.65 and 80.42%, respectively. Optimal transport efficiency occurs when the membrane thickness is moderate, neither too thin nor too thick, enabling faster, more balanced transport.

A membrane that is too thin can hinder transport due to the limited number of carriers, leading to competition among MG molecules for carrier interaction and reducing overall transport efficiency. On the other hand, an excessively thick membrane can also decrease transport efficiency, as the higher plasticizer content can slow the movement of MG through the membrane, limiting the amount that reaches the receiving phase.

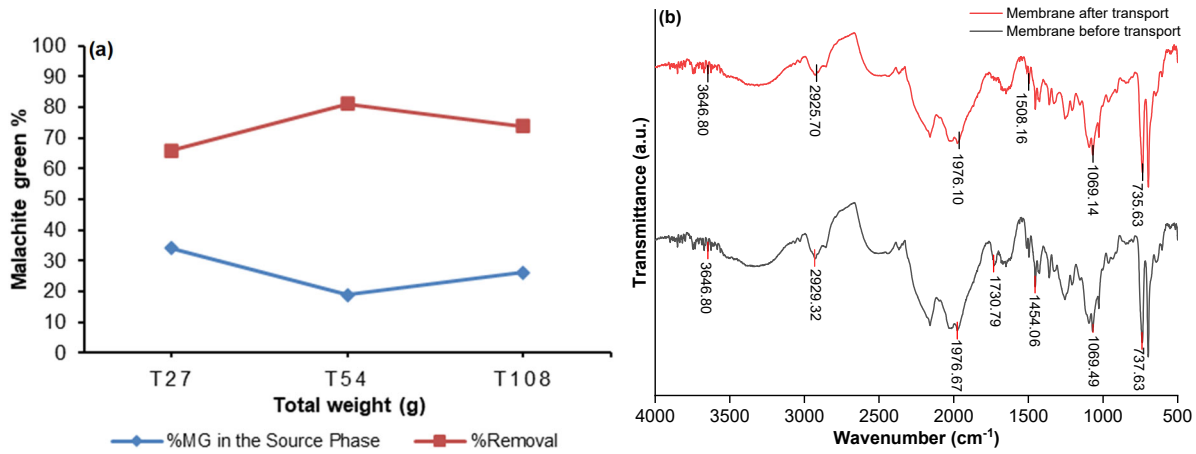

Fig 4. (a) Effect of PIM thickness on MG concentration and (b) FTIR spectra of the membrane at different thicknesses

FTIR characterization of the PIM membrane before and after MG transport at the optimum membrane thickness is shown in Fig. 4(b). The FTIR spectra present a comparison of the liquid membrane characteristics before and after the transport process of MG dye, with membrane thickness as the main variable. In the spectrum before transport, absorption bands are identified at 3647 cm^{-1}, corresponding to O–H stretching vibrations, 2929 cm^{-1} attributed to C–H stretching of alkyl groups, and 1976 cm^{-1} associated with combination bands or overtones. Other important bands include 1510 cm^{-1}, related to the stretching of double bonds in aromatic rings, 1069 cm^{-1} corresponding to C–N stretching, and a band at 737 cm^{-1} indicating deformation vibrations of aromatic structures.

Plasticizer plays a critical role in forming and solidifying the membrane structure. A low plasticizer content decreases membrane viscosity, while a high content increases it [27]. Excessive plasticizer can clog membrane pores, impeding MG diffusion and, consequently, reducing the transport percentage as viscosity increases [28]. In this study, dibenzyl ether used as a plasticizer may have blocked pores up to the membrane surface, hindering effective contact between MG and the active groups of the copolyeugenol diallyl phthalate carrier. Thus, within certain limits, an increase in membrane thickness can enhance the selectivity and stability of the membrane during the separation of ions and organic compounds such as MG [29].

Effect of Variation in Carrier Concentration on MG Transport

In this study, variations in the concentration of the carrier Co-EDAF 10% were conducted to evaluate its effect on the transport process of MG through the liquid membrane. The carrier concentrations used were 1×10^{-2}, 2×10^{-2}, 3×10^{-2}, 4×10^{-2}, and 5×10^{-2} M. It is expected that the higher the concentration of the carrier, the greater the amount of MG that can be transported.

The transport process was carried out using a source phase at pH 9, a receiving phase containing HNO_3 at 0.75 M, and a membrane with a T_{54} thickness. The results of the carrier concentration variation are presented in Fig. 5. Fig. 5(a) shows that the optimum carrier concentration for MG transport is 3×10^{-2} M, with a removal percentage of 86.20%. For Co-EDAF 10% concentrations of 1×10^{-2}, 2×10^{-2}, and 3×10^{-2} M, fluctuations in %removal are observed due to the increasing amount of copolyeugenol diallyl phthalate particles. This increase provides more available –OH active sites, enhancing hydrogen bonding interactions between MG and copolyeugenol diallyl phthalate 10%.

However, at higher concentrations, namely 4×10^{-2} and 5×10^{-2} M, the transport efficiency decreases. This reduction is attributed to an excess of copolyeugenol diallyl phthalate, with 10% active sites that are not proportional to the number of MG molecules, leading to the accumulation of active sites on the membrane surface, which in turn inhibits effective interaction. As a result,

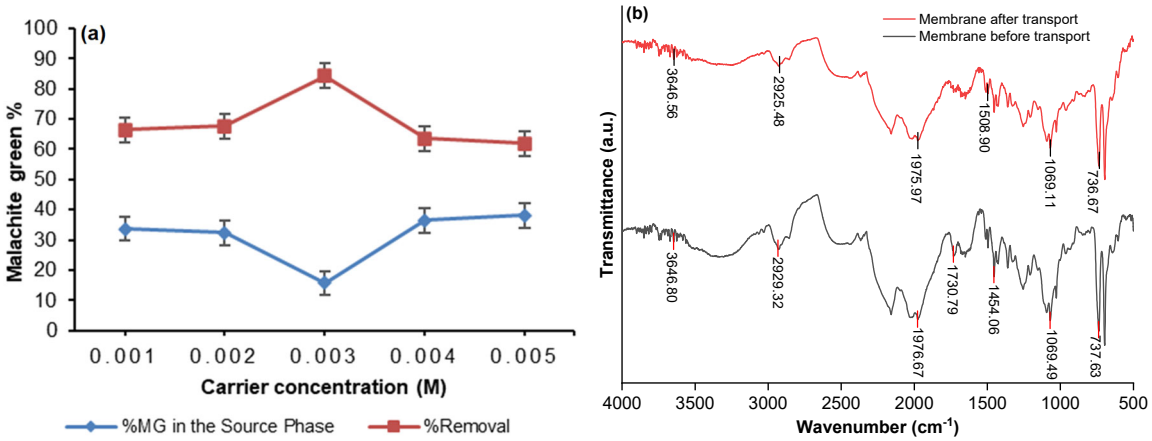

Fig 5. (a) Effect of carrier concentration on MG transport and (b) FTIR spectra at different carrier concentrations

competition between carrier molecules occurs, reducing the number of successful MG–carrier interactions and, in turn, decreasing the amount of MG transported.

Fig. 5(b) shows FTIR spectra comparing the characteristics of the liquid membrane before and after the MG transport process using variations in carrier concentration. The spectrum before transport displays characteristic absorption bands at 3647 cm^{-1}, representing the stretching vibration of O–H groups, 2929 cm^{-1} corresponding to C–H stretching of alkyl groups, and a band at 1510 cm^{-1} associated with aromatic vibrations of the benzene ring. In addition, the band at 1069 cm^{-1} indicates the presence of secondary amine groups or compounds containing C–N bonds.

The presence of carrier compounds in the membrane tends to enhance its ability to capture and transport dissolved substances, as the carrier functions as a complexing agent that facilitates selective binding to the target compound. This effectiveness strongly depends on the balance between the amount of carrier and the solubility of the target compound, so the optimal concentration must be determined experimentally. These findings are consistent with the statement by Kiswandono et al. [17], who emphasized that the carrier plays a crucial role in increasing both the selectivity and efficiency of the separation process in liquid membrane systems.

Effect of Variation in Transport Time on MG Transport

This study investigated the transport of MG as the contact time was varied. The experiments were conducted under optimal conditions, including the source phase pH, the HNO_3 concentration in the receiving phase, and the predetermined membrane thickness. It was expected that longer transport times would enhance the interaction between MG and the carrier within the membrane, thereby increasing the amount of MG transferred to the receiving phase. The transport process was carried out over 4, 8, 12, 18, and 24 h using 10% copolyeugenol diallyl phthalate as the carrier agent in the PIM. The effect of transport time variation on MG transport is presented in Fig. 6.

Fig. 6 shows that the optimal transport time is 12 h, with a MG removal percentage of 88.28%. Increasing the transport time increases the amount of MG transferred, as a longer interaction between MG and the carrier within the membrane enhances the release of ions into the receiving phase [30]. At a transport time of 4 h, only 79.56% of MG was successfully transferred, indicating

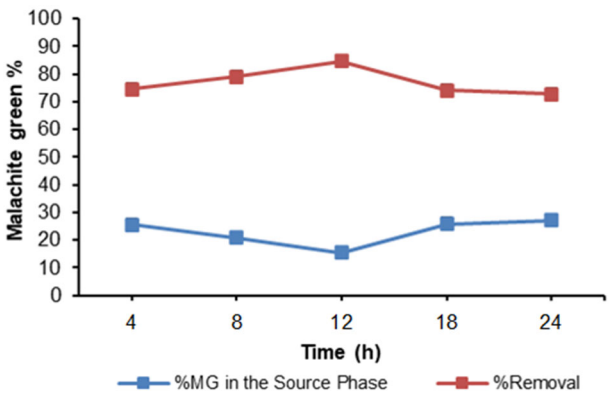

Fig 6. Effect of transport time variation on the concentration of transferred MG

that shorter transport durations improve efficiency. At 8 h, the transport percentage increased to 83.58% and continued to rise until reaching the optimal time.

After 12 h, the transport efficiency began to decline, as indicated by the data at 18 and 24 h, where only 79.22 and 78.18% of MG were successfully transferred, respectively. This decrease is attributed to the saturation of HNO_3 in the receiving phase, which hampers its ability to bind additional MG ions. According to Velikova et al. [31], the concentration gradient between the source and receiving phases diminishes over time, reducing the driving force for ion transport. As time progresses, the liquid membrane is also prone to component loss (leaching), including DBE, PVC, or the carrier. During transport, interfacial tension and contact angle may decrease due to membrane-solution interfacial contamination, chelating agent degradation, and other contributing factors [32].

Characterization by SEM is shown in Fig. 7, which illustrates the surface morphology of the PIM before and after the transport process. In the membrane before transport, the surface appears to be covered by the plasticizer, which functions as the liquid medium. After transport, the PIM morphology reveals cavities and large pores. The surface appears uneven and filled with visible pores. This condition is attributed to the porous nature of the PIM as a liquid membrane, where pores form due to the loss of membrane components during transport (leaching) and possible leakage, resulting in enlarged, more distinct pores.

Fig. 7 shows the surface morphology of the PIM before and after the transport process. Prior to transport, the membrane surface appeared to be coated with plasticizer, which acts as the liquid medium. After transport, observations revealed cavities and large pores on the membrane surface. The PIM surface post-transport appeared uneven and highly porous. This phenomenon occurs because PIM is a porous liquid membrane, in which pores form due to the loss of membrane components during transport (leaching) and leakage. This leakage leads to the enlargement of membrane pores, making them clearly visible.

Several studies have reported that, after transport, membranes can develop new cavities or pores due to the leaching of membrane components, such as plasticizers or carriers. For example, a study on Cr(VI) transport using ionic polymer inclusion membranes reported that the presence of room temperature ionic liquids (RTILs) in the membrane matrix can induce morphological and structural changes during the transport process, which subsequently affects membrane performance [33]. In addition, research on PIMs for MG using eugenol–diallyl phthalate copolymer also reported that the use of plasticizers in the membrane can block pores, hinder diffusion, and affect transport efficiency. Thus, the pore changes observed by SEM are consistent with the literature, indicating that the dye transport process affects not only the efficiency but also the membrane's physical structure.

PIM Lifetime

Lifetime testing was conducted to assess the stability of the PIM, both in the presence and absence of salts. Membrane stability was tested under various conditions:

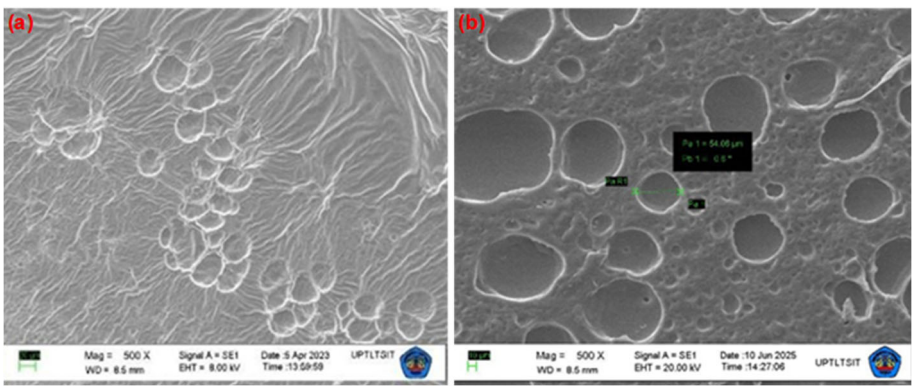

Fig 7. Surface morphology of PIM (a) before transport and (b) after 12 h of transport

without salt addition and with the addition of NaCl, Na_2SO_4, KNO_3, and $NaNO_3$, each at a concentration of 0.01 M. The addition of $NaNO_3$ resulted in the longest lifespan of the PIM membrane, reaching 69 days, compared to membranes without salt or with other salts. Previous studies have stated that membranes with higher stability tend to have a longer lifespan. A membrane is considered stable if it has a long service life, while leakage is indicated by the source phase pH approaching ±5 [34]. The relationship between the source phase pH and membrane lifetime is illustrated in Fig. 8.

The PIM membrane lifetime graph shows that membrane life increased up to 69 days with the addition of $NaNO_3$. This salt helped reduce LM loss by minimizing migration of the organic phase from the membrane, thereby improving membrane durability and lifespan. The competitive interaction between salt ions and MG molecules in binding water molecules triggered precipitation via a salting-out mechanism. Salting-out is a purification method that relies on the reduced solubility of compounds in high-ionic-strength solutions. The formation of precipitates helped slow membrane leakage, extending its operational life. In contrast, membranes without salt did not form precipitates, keeping membrane pores open. These open pores accelerated leakage and caused the pH of the source phase to rise more rapidly. The presence of such pores also accelerated the leakage rate, thereby reducing the membrane's lifespan. Under conditions with low or no salt concentration, emulsion formation was easier, resulting in lower PIM stability, increased LM loss, and reduced membrane lifespan. Conversely, the higher the concentration of added $NaNO_3$, the more difficult it was for emulsions to form, thereby improving PIM stability [11]. FTIR spectra of the PIM membrane before and after MG transport during lifetime testing is shown in Fig. 9.

Characterization results showed no significant wavelength shifts in the PIM membrane before or after the transport process. The specific absorption spectra in Fig. 9 indicated that the functional groups present in the PIM membrane after transport remained the same as those before transport. Therefore, the characterization analysis focused on changes in absorption intensity in the FTIR spectra. A decrease in FTIR absorption intensity

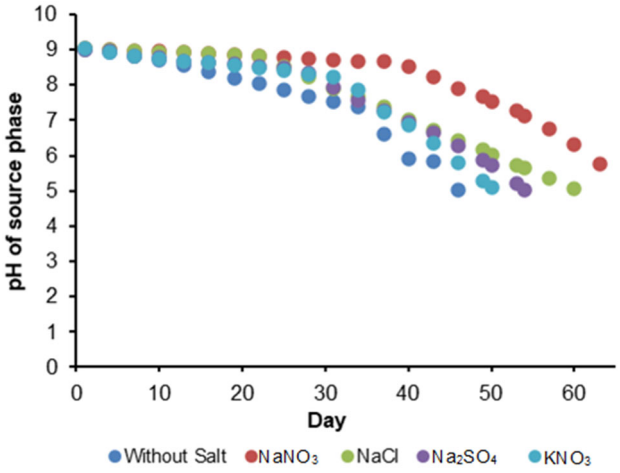

Fig 8. pH Lifetime measurement

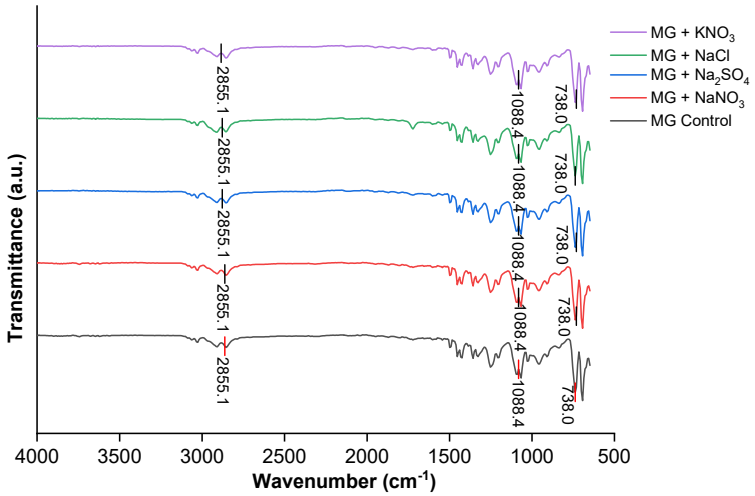

Fig 9. FTIR spectra of membrane lifetime for MG control, MG + $NaNO_3$, MG + Na_2SO_4, MG + NaCl, and MG + KNO_3

after transport indicated the loss of active membrane components or leaching into the receiving phase. A comparison of FTIR spectra before and after transport revealed reduced intensity at the –OH peak, indicating that –OH groups in the membrane leached into the receiving phase. This suggests that interactions occurred between the carrier and active membrane sites during the transport process. Since both MG and the carrier contain –OH groups, the potential for hydrogen bonding between them is high.

Leaching occurred due to interactions between MG and the carrier within the PIM membrane, involving hydrogen bonding and π-π interactions. The absence of detectable shifts in –OH functional groups, C sp^3–H (-CH_3) stretching, aromatic –C=C double bonds, (C–H) bending, and aromatic ring (C–H) vibrations indicated no direct interaction between salts and MG. The similar spectral patterns of the membrane before and after transport, as shown in Fig. 9, support this observation. The abundance of identical functional groups in the polymer structure is determined by infrared spectroscopy, which reveals changes in the relative intensities of absorption bands. Therefore, the differences between the two spectra lie only in the peak intensities or areas [11].

In this study, membrane lifetime testing was conducted by adding four different types of salts to the source phase: Na_2SO_4, NaCl, $NaNO_4$, and KNO_3, along with a control condition without added salt. After transport, the membrane was characterized by FTIR, and the results were compared with those of the membrane before transport to identify changes in functional groups and determine which components were lost. The results showed that the optimal membrane lifespan was achieved when $NaNO_3$ was added to the source phase. Based on FTIR analysis, the spectrum intensity of the membrane with $NaNO_3$ addition was similar to that of the control membrane, indicating that $NaNO_3$ has a better wavenumber absorption capability compared to other salts.

■ CONCLUSION

The optimal transport conditions for MG were achieved at a source-phase pH of 9, a receiving-phase HNO_3 concentration of 0.75 M, a medium-thickness membrane (T_{54}), and a transport duration of 18 h. Under these conditions, the transport efficiency of MG reached 84.60%, indicating that the copolyeugenol diallyl phthalate 10%-based PIM liquid membrane system is effective for the selective separation of the MG dye. The membrane lifetime reached 69 days, particularly when $NaNO_3$ was added to the source phase. FTIR characterization results showed a decrease in membrane spectral intensity after transport, indicating the loss of membrane components (leaching). This finding is supported by SEM characterization, which revealed the formation of pores on the membrane surface after transport, further indicating the loss of membrane components (leaching). The membrane maintained over 80% of its initial transport efficiency after five consecutive cycles, suggesting a longer operational lifespan than previously reported PIMs. These results highlight that the present study not only optimizes transport conditions but also provides a membrane with enhanced performance, stability, and durability, thereby contributing significant novelty to the field.

■ ACKNOWLEDGMENTS

The author would like to thank the Institute for Research and Community Service (LPPM) of the University of Lampung for funding the Professorship Research under Contract Number 699/UN26.21/PN/2025 dated June 2, 2025.

■ CONFLICT OF INTEREST

The authors have no conflict of interest.

■ AUTHOR CONTRIBUTIONS

Rusyda Maulida Khairati conducted the experiment and wrote the manuscript. Agung Abadi Kiswandono, as the supervisor, revised the manuscript. Rinawati revised the manuscript. Ni Luh Ratna Gede Juliasih contributed to the data curation. Mita Rilyanti reviewed the paper. Ilim reviewed the paper. Annur Valita Sindiani did the characterization and also edited the manuscript. Herlian Eriska Putra revised the substantial content. All authors agreed to the final version of this manuscript.

■ REFERENCES

[1] Ling, Y.Y., and Mohd Suah, F.B., 2017, Extraction of malachite green from wastewater by using polymer inclusion membrane, *J. Environ. Chem. Eng.*, 5 (1) 785–794.

[2] Taufik, R., Mohamad, M., Wannahari, R., Shoparwe, N.F., Osman, W.H.W., Teo, P.T., and Masri, M.N., 2021, Spent coffee ground as low-cost adsorbent for Congo red dye removal: Optimization and kinetics, *IOP Conf. Ser.: Earth Environ. Sci.*, 765 (1), 012089.

[3] Yuningsih, N.E., Ariani, L., Suprapto, S., Ulfin, I., Harmami, H., Juwono, H., and Ni'mah, Y.L., 2024, Adsorption of malachite green using activated carbon from mangosteen peel: Optimization using Box-Behnken design, *J. Renewable Mater.*, 12 (5), 981–992.

[4] Benosmane, N., Boutemeur, B., Hamdi, S.M., and Hamdi, M., 2018, Removal of phenol from aqueous solution using polymer inclusion membrane based on mixture of CTA and CA, *Appl. Water Sci.*, 8 (1), 17.

[5] Soo, J.A.L., Makhtar, M.M.Z., Shoparwe, N.F., Otitoju, T.A., Mohamad, M., Tan, L.S., and Li, S., 2021, Characterization and kinetic studies of poly(vinylidene fluoride-co-hexafluoropropylene) polymer inclusion membrane for the malachite green extraction, *Membranes*, 11 (9), 676.

[6] Saka, C., Kiswandono, A.A., and Hadi, S., 2020, Synthesis of polymer inclusion membranes based on PVC containing copoly-EDVB 4% as a carrier for removal of phenol solutions, *Pollut. Res.*, 39 (4), 1009–1016.

[7] Chauke, N.M., Munonde, T.S., and Mketo, N., 2025, A critical review of the anti-biofouling properties of biogenic-based silver nanoparticles (AgNPs) embedded on polymer membranes for wastewater treatment, *J. Ind. Eng. Chem.*, 149, 209–232.

[8] Macías, M., and Rodríguez de San Miguel, E., 2023, On the use of polymer inclusion membranes for the selective separation of Pb(II), Cd(II), and Zn(II) from seawater, *Membranes*, 13 (5), 512.

[9] Husna, S.M., Yusoff, A.H., Mohan, M., Azmi, N.A., Ter, T.P., Shoparwe, N.F., and Sulaiman, A.Z., 2022, Effect of graphene oxide on the properties of polymer inclusion membranes for gold extraction from acidic solution, *Membranes*, 12 (10), 996.

[10] Kiswandono, A.A., Nusantari, C.S., Rinawati, R., and Hadi, S., 2022, Optimization and evaluation of polymer inclusion membranes based on pvc containing copoly-EDVB 4% as a carrier for the removal of phenol solutions, *Membranes*, 12 (3), 295.

[11] Sun, H., Yao, J., Li, D., Li, Q., Liu, B., Liu, S., Cong, H., Sjak, V., and Feng, C., 2017, Removal of phenols from coal gasification wastewater through polypropylene hollow fiber supported liquid membrane, *Chem. Eng. Res. Des.*, 123, 277–283.

[12] Kaczorowska, M.A., Bożejewicz, D., and Witt, K., 2023, The application of polymer inclusion membranes for the removal of emerging contaminants and synthetic dyes from aqueous solutions — A mini review, *Membranes*, 13 (2), 132.

[13] Jayanayak, G.M., Ganalu, R., Shashikanth, S., Ukkund, S.J., Ahmed, S., AlSubih, M., and Islam, S., 2024, Studies on the removal of malachite green from its aqueous solution using water-insoluble β-cyclodextrin polymers, *ACS Omega*, 9 (9), 10132–10145.

[14] Fadlelmoula, A., Pinho, D., Carvalho, V.H., Catarino, S.O., and Minas, G., 2022, Fourier transform infrared (FTIR) spectroscopy to analyse human blood over the last 20 years: A review towards lab-on-a-chip devices, *Micromachines*, 13 (2), 187.

[15] Khairati, R.M., Kiswandono, A.A., and Ma'ruf, D.I., 2025, Application of polymer inclusion membrane in the transport of malachite green dye using copolymer (eugenol-diallyl phthalate) 2% as a carrier, *J. Kim. Sains Apl.*, 28 (1), 8–15.

[16] Chen, X., and Holze, R., 2024, Polymer electrolytes for supercapacitors, *Polymers*, 16 (22), 3164.

[17] Kiswandono, A.A., Sindiani, A.V., Khotimah, R.K., Rabbani, M.B., Kurniawan, B., Rinawati, R., and Putra, H.E., 2024, Transport of malachite green using the polyeugenol-based polymer inclusion membrane (PIM) method, *J. Membr. Sci. Res.*, 10 (1), 2013382.

[18] Kozlowski, C., and Zawierucha, I., 2025, Polymer inclusion membranes based on sulfonic acid derivatives as ion carriers for selective separation of Pb(II), Cu(II) and Cd(II) ions, *Membranes*, 15 (5), 146.

[19] Ashraf, W.M., Abulibdeh, N., and Salam, A., 2019, Selective removal of malachite green dye from aqueous solutions by supported liquid membrane technology, *Int. J. Environ. Res. Public Health*, 16 (18), 3484.

[20] Zulkefeli, N.S.W., Weng, S.K., and Abdul Halim, N.S., 2018, Removal of heavy metals by polymer inclusion membranes, *Curr. Pollut. Rep.*, 4 (2), 84–92.

[21] Ahmad, A.A., Ahmad, M.A., Yahaya, N.K.E.M., and Karim, J., 2021, Adsorption of malachite green by activated carbon derived from gasified *Hevea brasiliensis* root, *Arabian J. Chem.*, 14 (10), 103104.

[22] Hoque, B., Almeida, M.I.G.S., Cattrall, R.W., Gopakumar, T.G., and Kolev, S.D., 2019, Effect of cross-linking on the performance of polymer inclusion membranes (PIMs) for the extraction, transport and separation of Zn(II), *J. Membr. Sci.*, 589, 117256.

[23] Senila, M., 2025, Polymer Inclusion membranes (PIMs) for metal separation—Toward environmentally friendly production and applications, *Polymers*, 17 (6), 725.

[24] Richard, E., Fatyeyeva, K., and Marais, S., 2025, Ionic liquid-based polymer inclusion membranes for heavy metal ions removal from water: Achievements and challenges, *Chem. Eng. J.*, 505, 158916.

[25] Adigun, B., Thapaliya, B.P., Luo, H., and Dai, S., 2024, Ionic liquid-based extraction of metal ions via polymer inclusion membranes: A critical review, *RSC Sustainability*, 2 (10), 2768–2780.

[26] Hadri, M., Draoui, K., Bounab, L., Hamdaoui, M., Douhri, H., Kouda, I., and Zaitan, H., 2022, Thermodynamic and kinetic studies for the adsorption of malachite green on diatomite, *J. Environ. Eng. Sci.*, 18 (2), 70–80.

[27] Kiswandono, A.A., Ningsih, N., Sindiani, A.V., Rinawati, R., and Qudus, H.I., 2024, Phenol solutions recovery as water pollutants with eugenol cross-linked diallyl phthalate using supported liquid membrane, *Global J. Environ. Sci. Manage.*, 10, 53–70.

[28] Szczepanski, P., Guo, H., Dzieszkowski, K., Rafiński, Z., Wolan, A., Fatyeyeva, K., Kujawa, J., and Kujawski, W., 2021, New reactive ionic liquids as carriers in polymer inclusion membranes for transport and separation of Cd(II), Cu(II), Pb(II), and Zn(II) ions from chloride aqueous solutions, *J. Membr. Sci.*, 638, 119674.

[29] Wang., D., Cattrall, R.W., Li, J., Almeida, M.I.G.S., Stevens, G.W., and Kolev, S.D., 2017, A poly(vinylidene fluoride-co-hexafluoropropylene) (PVDF-HFP)-based polymer inclusion membrane (PIM) containing LIX84I for the extraction and transport of Cu(II) from its ammonium sulfate/ammonia solutions, *J. Membr. Sci.*, 542, 272–279.

[30] Radzymińska-Lenarcik, E., Kwiatkowska-Marks, S., and Kościuszko, A., 2022, Transport of heavy metals Pb(II), Zn(II) and Cd(II) ions across CTA polymer membranes containing alkyl-triazole as ion carriers, *Membranes*, 12 (11), 1068

[31] Velikova, K., Dudev, T., Sarafska, T., Kukoc-Modun, L., Kolev, S.D., and Spassov, T., 2025, Assessing the stability of polymer inclusion membranes: The case of aliquat 336-based membranes, *Membranes*, 15 (10), 309.

[32] Zioui, D., Aoudjit, L., Tigrine, Z., Aburideh, H., and Arous, O., 2022, Competitive transport of metal ions through a PVDF-CTA based polymer inclusion membrane containing D_2EHPA as carrier, *Russ. J. Phys. Chem. A*, 96 (6), 1334–1339.

[33] Turgut, H.I., Eyupoglu, V., Kumbasar, R.A., and Sisman, I., 2017, Alkyl chain length dependent Cr(VI) transport by polymer inclusion membrane using room temperature ionic liquids as carrier and PVDF-co-HFP as polymer matrix, *Sep. Purif. Technol.*, 175, 406–417.